

SAKED: Mitigating Hallucination in Large Vision-Language Models via Stability-Aware Knowledge Enhanced Decoding

Zhaoxu Li ^{*1,2} Chenqi Kong ^{*1} Peijun Bao ¹ Song Xia ¹ Yi Tu ³ Yi Yu ¹
 Xinghao Jiang ⁴ Xudong Jiang ¹

Abstract

Hallucinations in Large Vision-Language Models (LVLMs) pose significant security and reliability risks in real-world applications. Inspired by the observation that humans are more error-prone when uncertain or hesitant, we investigate how instability in a model’s internal knowledge contributes to LVLM hallucinations. We conduct extensive empirical analyses from three perspectives, namely attention heads, model layers, and decoding tokens, and identify three key hallucination patterns: (i) visual activation drift across attention heads, (ii) pronounced knowledge fluctuations across layers, and (iii) visual focus distraction between neighboring output tokens. Building on these findings, we propose **Stability-Aware Knowledge-Enhanced Decoding (SAKED)**, which introduces a layer-wise **Knowledge Stability Score (KSS)** to quantify knowledge stability throughout the model. By contrasting the most stability-aware and stability-agnostic layers, SAKED suppresses decoding noise and dynamically leverages the most reliable internal knowledge for faithful token generation. Moreover, SAKED is training-free and can be seamlessly integrated into different architectures. Extensive experiments demonstrate that SAKED achieves state-of-the-art performance for hallucination mitigation on various models, tasks, and benchmarks.

1. Introduction

In recent years, Large Vision-Language Models (LVLMs) have made substantial progress in cross-modal understanding and generation. By connecting a pretrained language model with a vision encoder and fine-tuning on instruction-based datasets, LVLMs achieve strong performance across a wide range of multimodal tasks (OpenAI, 2023; Chen et al., 2023; Yin et al., 2024; Zhao et al., 2024b). Nevertheless, LVLMs remain prone to hallucinations (Rohrbach et al., 2018; Zhou et al., 2023; Li et al., 2023b), where models generate content that is not grounded in the input signals but instead relies on their internal knowledge (Heiman et al., 2025). Such failures raise pressing safety and security concerns in high-stakes applications, such as autonomous driving, medical diagnosis, and financial analysis, etc (Li et al., 2026; Zhang et al., 2023; Xia et al., 2026).

Prior work has investigated the causes of LVLM hallucinations, including language priors (Wang et al., 2024a; Li et al., 2026), dataset bias (Li et al., 2023b; Zhou et al., 2023), error accumulation (Huang et al., 2024; Zhou et al., 2023), and suboptimal training policy (Kalai et al., 2025; Yang et al., 2025). Accordingly, a variety of mitigation strategies have been proposed, such as contrastive decoding (Leng et al., 2024; Favero et al., 2024; Chuang et al., 2023), fine-tuning with improved learning policies (Jiang et al., 2024; Yang et al., 2025; Sarkar et al., 2025), early intervention (Wang et al., 2024a; Li et al., 2026; Wang et al., 2025a), information steering (Li et al., 2025; Park et al., 2025a), and representation editing (Liu et al., 2024; Kang et al., 2025; Gong et al., 2024; Kong et al., 2025). Despite this progress, most existing methods do not explicitly model how internal knowledge fluctuations give rise to hallucinations. Without characterizing when and where internal knowledge becomes unreliable, mitigation methods can be brittle and may fail under distribution shifts (Heiman et al., 2025; Lv et al., 2024). In contrast, a stability-aware perspective enables the model to dynamically leverage more reliable internal knowledge, thereby achieving more faithful decoding.

Inspired by the observation that humans are more error prone when uncertain or hesitant, we investigate hallucinations in LVLMs through the lens of internal knowledge

^{*}Equal contribution. ¹ROSE Lab, School of Electrical and Electronic Engineering, Nanyang Technological University, Singapore ²ROSE Lab, Interdisciplinary Graduate Programme, Nanyang Technological University, Singapore ³School of Physical and Mathematical Sciences, Nanyang Technological University, Singapore ⁴Shanghai Jiao Tong University, China. Correspondence to: <>.

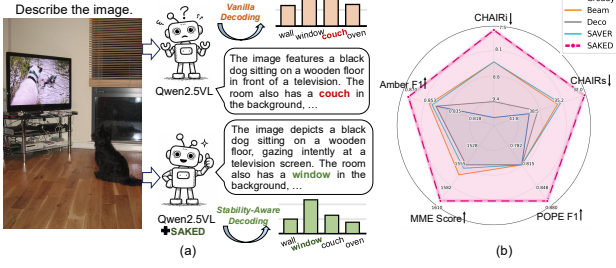


Figure 1. (a) SAKED mines internal stability-aware knowledge to enhance the decoding process. (b) SAKED consistently achieves outstanding hallucination performance on CHAIR, POPE, MME, and AMBER.

stability. A key challenge is to explicitly characterize and quantify knowledge fluctuation during generation. To this end, we conduct extensive empirical analyses of knowledge stability from three perspectives: attention heads, model layers, and decoding tokens. These analyses reveal three stability patterns associated with hallucinations. **Pattern #1:** Visual activation drifts across attention heads can induce hallucinations; in contrast, heads with consistent visual activations exhibit stronger visual grounding and yield more faithful decoding. **Pattern #2:** Large knowledge fluctuations across layers correlate with higher hallucination risk, whereas stable layers preserve more reliable information during token generation. **Pattern #3:** Substantial distraction in visual focus between neighboring output tokens also increases likelihood of hallucinations.

We propose Knowledge Stability Score (KSS), which comprises (i) Cross-Head Stability Score (CHSS) to measure visual activation drift across attention heads, (ii) Cross-Layer Stability Score (CLSS) to quantify knowledge fluctuations across layers, and (iii) Cross-Token Stability Score (CTSS) to assess visual focus distraction between adjacent decoding steps. Building on KSS, we further introduce stability-aware contrastive decoding that contrasts logits from the most stability-aware layer and the most stability-agnostic layer to suppress decoding noise and improve faithfulness. As shown in Figure 1, SAKED consistently outperforms prior methods by a clear margin across multiple tasks. In summary, our main contributions are as follows:

- We conduct extensive empirical analyses to examine when and where hallucinations arise by tracking model knowledge evolution from three perspectives: attention heads, model layers, and generated tokens. We find that unstable internal model knowledge is associated with a higher risk of hallucination.
- We propose a novel **Stability-Aware Knowledge Enhanced Decoding (SAKED)** method that quantifies knowledge stability for each layer. We further improve decoding by contrasting the most stability-aware layer with the most stability-agnostic layer, thereby reducing

hallucinations. SAKED is plug-and-play and can be seamlessly integrated into various LVLMs.

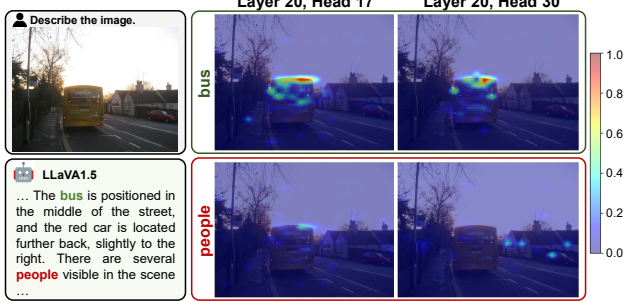


Figure 2. The left panel shows the input image and the output caption. The right panel visualizes the attention maps of a grounded token (“bus”) and a hallucinated token (“people”) across different attention heads.

- Extensive experiments demonstrate that SAKED achieves state-of-the-art hallucination mitigation performance across a wide range of models, datasets, and tasks.

2. Related Work

2.1. Large Vision-Language Models (LVLMs)

Recent advances in LVLMs have yielded strong performance across a wide range of vision–language tasks. Most LVLMs consist of three components: a vision encoder that extracts visual features from the input image, a vision–language connector that aligns these features with the language representation space, and a pretrained LLM that consumes the resulting multimodal embeddings to generate responses. To reduce the modality gap between visual features and textual representations, prior work has explored diverse alignment strategies, including lightweight linear projection layers that map visual features into the LLM token space (e.g., LLaVA (Liu et al., 2023), MiniGPT-4 (Zhu et al., 2023)), Q-former modules that learn query embeddings for multimodal grounding (e.g., BLIP-2 (Li et al., 2023a), InstructBLIP (Dai et al., 2023)), and cross-attention architectures that enable iterative interaction between visual tokens and text (e.g., Flamingo (Alayrac et al., 2022), OpenFlamingo (Awadalla et al., 2023)). More recent systems, such as GPT-5 (OpenAI, 2025) and Gemini-3 (Google DeepMind, 2025), further demonstrate enhanced capabilities on vision tasks requiring complex reasoning. Despite this progress, LVLMs remain susceptible to severe hallucinations, raising pressing safety and security concerns, especially in critical application scenarios (e.g., medical diagnosis).

2.2. Hallucination in LVLMs

Hallucination in LVLMs typically refers to outputs that are not grounded in the input signals and instead rely excess-

sively on the model’s internal knowledge (Heiman et al., 2025). Recent tuning-based approaches usually improve their learning objectives or training policies (Jiang et al., 2024; Yang et al., 2025; Sarkar et al., 2025; Park et al., 2025b; Xu et al., 2024; He et al.) on high-quality curated datasets (Wang et al., 2024b; Zhang et al., 2024; Jing & Du, 2024). In contrast, training-free methods are generally more computationally efficient. For example, contrastive decoding (Leng et al., 2024; Favero et al., 2024; Chuang et al., 2023; Zhu et al.) compares output logits across paired inputs (e.g., different image conditions) to suppress ungrounded generations. Early-intervention approaches (Wang et al., 2024a; Li et al., 2026; Wang et al., 2025a; Chen et al., 2024b; Wu et al., 2024; Fang et al., 2025a; Wang et al., 2025b; Fang et al., 2025b) dynamically refine decoding by leveraging more reliable signals from earlier layers. In addition, representation-editing methods (Liu et al., 2024; Kang et al., 2025; Gong et al., 2024; Zhao et al., 2024a; Zou et al., 2024; Chen et al., 2024a; Tan et al., 2025) reallocate attention to encourage the model to focus on relevant visual regions. Despite substantial progress, the role of internal knowledge stability in mitigating hallucinations remains underexplored. To address this gap, we propose SAKED, which mines stability-aware knowledge within LVLMs to dynamically enhance decoding and reduce hallucinations.

3. Methodology

In this section, we study how instability in internal model knowledge contributes to hallucinations in LVLMs. We first formalize the LVLM generation process and introduce the necessary notations. We then analyze the relationship between knowledge stability and hallucination from three perspectives: attention heads, model layers, and decoding steps. Our empirical studies identify three key factors contributing to hallucinations: visual activation drift across attention heads, knowledge fluctuations across layers, and visual focus distraction between adjacent steps. Based on these observations, we propose **Stability-Aware Knowledge Enhanced Decoding (SAKED)**. To quantify stability-aware knowledge, we design three metrics: Cross-Head Stability Score (CHSS), Cross-Layer Stability Score (CLSS), and Cross-Token Stability Score (CTSS). Finally, we identify stability-aware (positive) and stability-agnostic (negative) layer pair and incorporate them into a contrastive decoding strategy that suppresses decoding noise and improves faithfulness. SAKED dynamically corrects generated tokens and can be flexibly adapted to different models in a plug-and-play manner.

3.1. Preliminaries

LVLMs typically consist of three key components: a vision encoder, a projection module, and an autoregressive language model. The vision encoder first converts

an input image into a sequence of visual tokens $\mathbf{x}^I = \{\mathbf{x}_1^I, \mathbf{x}_2^I, \dots, \mathbf{x}_m^I\}$. In parallel, a text prompt is tokenized into n textual tokens $\mathbf{x}^P = \{\mathbf{x}_1^P, \mathbf{x}_2^P, \dots, \mathbf{x}_n^P\}$. Here m and n are the lengths of the visual and textual tokens. The visual and textual embeddings are concatenated to form the model input \mathbf{x} , which is passed through an autoregressive language model composed of L stacked transformer decoder layers. At each layer l , the model produces hidden states $\mathbf{h}^l = \{\mathbf{h}_0^l, \mathbf{h}_1^l, \dots, \mathbf{h}_{m+n-1}^l\}$. During generation, the hidden state at the final position \mathbf{h}_{m+n-1}^L is projected via an affine transformation $\phi(\cdot)$ to produce a probability distribution over the vocabulary \mathcal{V} (θ represents the LVLM parameters):

$$\mathbf{y}_t \sim p_\theta(\mathbf{y}_t | \mathbf{x}^I, \mathbf{x}^P, \mathbf{y}_{<t}) \quad (1)$$

3.2. Visual Activation Drift across Attention Heads Induces Hallucinations

We first examine the relationship between cross-head knowledge consistency and hallucination. In transformers, multi-head self-attention aggregates multiple “attention views” to form more robust representations. Figure 2 visualizes the visual activations of a grounded token (“bus”) and a hallucinated token (“people”) across attention heads within a single layer. The grounded token “bus” exhibits concentrated high-activation regions that align with its semantic meaning, whereas the hallucinated token “people” shows diffuse, higher-entropy activations. Moreover, the grounded token demonstrates stronger cross-head consistency in its activated regions than the hallucinated token. Together, these observations suggest that hallucinations are more likely when visual information varies substantially across attention heads. Motivated by these observations, we first define the Visual Activation Score (VAS) to quantify the activation strength and concentration level of the k -th attention head:

$$\text{VAS}_t^{(l,k)} = M_t^{(l,k)} + O_t^{(l,k)} \quad (2)$$

At each generation step t , $M_t^{(l,k)}$ and $O_t^{(l,k)}$ denote the maximum value and entropy of visual attention map $A_t^{(l,k)} \in \mathbb{R}^{a \times a}$ in layer l , respectively. Heads with higher VAS are expected to be more informative and reliable. As such, for each layer l , we select the K most representative heads $\hat{A}_t^{(l,k)}$ with the highest $\text{VAS}_t^{(l,k)}$ values from H heads, where $k \in \mathcal{K}$ and $\mathcal{K} = \{1, \dots, K\}$. We further define the Cross-Head Stability Score (CHSS) to measure knowledge stability across attention heads:

$$\text{CHSS}_t^l = \frac{1}{K(K-1)} \sum_{s, k \in \mathcal{K}, s < k} \text{SoftIoU}(\hat{A}_t^{(l,s)}, \hat{A}_t^{(l,k)}) \quad (3)$$

We introduce SoftIoU to quantify the consistency between two selected heads s and k (We omit the subscript t for

brevity):

$$\text{SoftIoU}(\hat{A}^{(l,s)}, \hat{A}^{(l,k)}) = \frac{\|\min(\hat{A}^{(l,s)}, \hat{A}^{(l,k)})\|_1}{\|\max(\hat{A}^{(l,s)}, \hat{A}^{(l,k)})\|_1 + \varepsilon}, \quad (4)$$

Here, $\min(\cdot)$ and $\max(\cdot)$ are applied element-wise at the corresponding spatial locations in the attention map, and ε is a small constant for numerical stability.

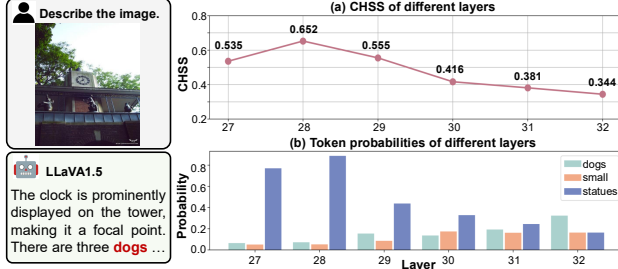


Figure 3. (a) CHSS distribution across model layers. (b) Token probability distributions across model layers. For clarity, we show only the three highest probability tokens in the final layer: “dogs”, “small”, and “statues”.

Figure 3 presents the layer-wise distribution of CHSS_t^l together with the corresponding token probability distributions across layers. For clarity, we show only the three highest probability tokens (i.e., “dogs”, “small”, and “statues”) in the final layer. We observe that higher CHSS values, such as those in layers 27 and 28, are associated with more accurate token predictions, indicating more consistent visual activation across heads. In contrast, the final layer exhibits the lowest CHSS and produces a hallucinated token. This observation motivates selecting the layer that contains the most stable knowledge to support more faithful token generation.

3.3. Knowledge Fluctuations across Layers Implies Hallucinations

In this subsection, we investigate how knowledge evolves and where knowledge instability happens across model layers. Figure 4 visualizes the Jensen-Shannon Divergence (JSD) of layer-wise logit distributions. The left panel shows a representative example evaluated by LLaVA-1.5, where the hallucinated token “people” is highlighted. For each generated token y_t , we apply LogitLens to the hidden state \mathbf{h}_t^l from each layer and obtain the corresponding token distribution:

$$\phi(\mathbf{h}_t^l) = \text{softmax}(\text{LogitLens}(\mathbf{h}_t^l)), \quad l \in L \quad (5)$$

LogitLens maps intermediate representations to the vocabulary space, enabling explicit visualization of how internal knowledge evolves across layers. We then define the Cross-Layer Stability Score (CLSS) by measuring the JSD

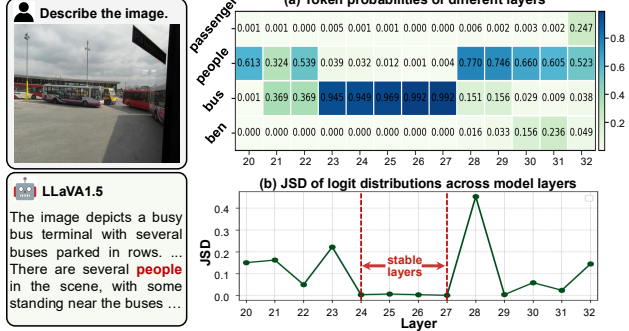


Figure 4. (a) Probability distributions of the generated token “people” across model layers (due to space limitations, we show the four highest-probability tokens in the final layer: “passengers”, “people”, “bus”, and “ben”); (b) JSD between the logit distributions of each layer and its adjacent layer, where lower JSD indicates a more stable flow of knowledge.

between consecutive layers:

$$\text{CLSS}_t^l = 1 - \text{JSD}(\phi(\mathbf{h}_t^l), \phi(\mathbf{h}_t^{l-1})) \quad (6)$$

Figure 4 (a) illustrates probability distribution of the current token y_t (“people”) changes across layers. Due to space limitations, we report only the four highest-probability tokens in the final layer (“passengers”, “people”, “bus”, and “ben”). Figure 4 (b) shows the JSD between adjacent layers, where lower values indicate more stable knowledge flow. Notably, the JSD increases sharply around layer 28, suggesting substantial internal knowledge fluctuation. In such cases, the model’s token preference becomes unstable across layers, which can lead to hallucinated outputs. We find that stable layer-to-layer transitions (layers 24-27) correlate with more faithful generations. Moreover, when hallucinations occur, the most stable transitions often appear in intermediate layers rather than in the final layer.

3.4. Visual Focus Distraction between Neighboring Tokens Triggers Hallucinations

We further investigate how knowledge instability manifests across sequential decoding steps and contributes to hallucinations. Motivated by the observation that neighboring tokens often refer to the same visual entity. For example, in the phrase “yellow bus”, both “yellow” and “bus” describe the entity bus. We thereby hypothesize that faithful decoding should maintain similar visual focus for adjacent tokens. Analogously, human decisions are more error-prone when attention is distracted. To test this hypothesis, we quantify Visual Focus Distraction (VFD) between consecutive generated tokens as the average JSD of their visual attention heads:

$$\text{VFD}_t^l = \frac{1}{|\mathcal{H}|} \sum_{h \in |\mathcal{H}|} \text{JSD}(A_t^{(l,h)}, A_{t-1}^{(l,h)}) \quad (7)$$

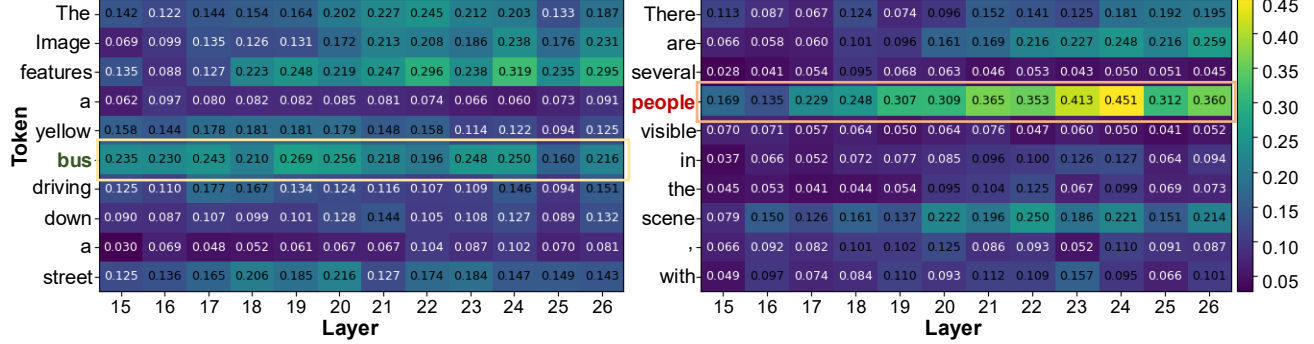


Figure 5. VFD distributions of visual attention between each token and its adjacent token across model layers. The grounded token “bus” and the hallucinated token “people” are highlighted in green and red, respectively. Compared to real tokens, the hallucinated token exhibits substantial visual focus distraction during decoding.

Algorithm 1 Stability-Aware Knowledge Enhanced Decoding (SAKED)

Require: Inputs $\{\mathbf{x}^I, \mathbf{x}^P\}$, candidate layers L_c , contrastive weight α , token revision weight β , score weights $\{\lambda_1, \lambda_2, \lambda_3\}$
 At every decoding step t :
for $l \in L_c$ **do**
 Calculate CHSS $_t^l$ using Eq. 3 **# Cross-Head Stability**
 Calculate CLSS $_t^l$ using Eq. 6 **# Cross-Layer Stability**
 Calculate CTSS $_t^l$ using Eq. 8 **# Cross-Token Stability**
 Overall Knowledge Stability Score (KSS):

$$\text{KSS}_t^l = \lambda_1 \text{CHSS}_t^l + \lambda_2 \text{CLSS}_t^l + \lambda_3 \text{CTSS}_t^l$$

end for
 Select positive layer l^+ and negative layer l^- :

$$l^+ = \underset{l \in L_c}{\text{argmax}} \text{KSS}_t^l, \quad l^- = \underset{l \in L_c}{\text{argmin}} \text{KSS}_t^l$$

 Contrastive Decoding:

$$\mathbf{y}_t^{\text{cont}} = \text{softmax}[(1 + \alpha)\text{logit}(\mathbf{h}_t^{l^+}) - \alpha\text{logit}(\mathbf{h}_t^{l^-})]$$

 Output Token Revision:

$$\hat{\mathbf{y}}_t = \mathbf{y}_t + \beta \mathbf{y}_t^{\text{cont}}$$

Figure 5 presents the VFD distributions of different tokens across layers. For the grounded token “bus”, the VFD remains consistently low, indicating that the model attends to consistent image regions when generating neighboring tokens. Its adjacent tokens “yellow” and “driving” exhibit similarly stable focus, consistent with their shared referent. In contrast, for the hallucinated token “people”, the model’s visual focus deviates from that of the preceding token, resulting in substantially higher VFD values, particularly in deeper layers. This elevated divergence suggests increased uncertainty during decoding and indicates that visual focus distraction in deeper layers is associated with a higher risk of hallucination. Finally, we define the Cross-Token Stability Score (CTSS) to quantify model’s temporal knowledge stability:

$$\text{CTSS}_t^l = 1 - \text{VFD}_t^l \quad (8)$$

3.5. Stability-Aware Knowledge Enhanced Decoding (SAKED)

We define the overall Knowledge Stability Score (KSS) as a weighted sum of the three stability metrics introduced above, thereby quantifying knowledge stability from the head-, layer-, and token-level perspectives:

$$\text{KSS}_t^l = \lambda_1 \text{CHSS}_t^l + \lambda_2 \text{CLSS}_t^l + \lambda_3 \text{CTSS}_t^l \quad (9)$$

The findings above indicate that internal knowledge stability varies across layers. Accordingly, we select the most stability-aware layer l^+ and the most stability-agnostic layer l^- based on KSS_t^l , forming a positive-negative layer pair:

$$l^+ = \underset{l \in L_c}{\arg \max} \text{KSS}^l; \quad l^- = \underset{l \in L_c}{\arg \min} \text{KSS}^l \quad (10)$$

We propose Stability-Aware Contrastive Decoding (SACD), which performs contrastive decoding by combining the logits computed from the hidden states $\mathbf{h}_t^{l^+}$ and $\mathbf{h}_t^{l^-}$ to obtain the next-token distribution:

$$\mathbf{y}_t^{\text{cont}} = \text{softmax}[(1 + \alpha)\text{logit}(\mathbf{h}_t^{l^+}) - \alpha\text{logit}(\mathbf{h}_t^{l^-})], \quad (11)$$

where α controls the contrast strength. Overall, stability-aware contrastive decoding suppresses decoding noise by dynamically leveraging the most reliable internal knowledge for faithful token generation. Finally, we dynamically adjust the output token by:

$$\hat{\mathbf{y}}_t = \mathbf{y}_t + \beta \mathbf{y}_t^{\text{cont}}, \quad \text{subject to } \hat{\mathbf{y}}_t \in \mathcal{V}_{\text{candidate}} \quad (12)$$

Here, \mathcal{V} is the whole vocabulary, and $\mathcal{V}_{\text{candidate}}$ indicates the top- q (default: $q=20$) tokens with the highest probability under the original distribution \mathbf{y}_t , because we empirically observe that the grounded token remains within this set even when the model produces a hallucinated output. The pipeline of SAKED is summarized in Algorithm 1.

Table 1. Hallucination evaluation results on CHAIR across five models. Ci and Cs represent CHAIRi and CHAIRs, respectively. (OPERA cannot be applied to Qwen2.5VL and InternVL3 due to architectural constraints)

Model	LLaVA1.5		InstructBLIP		MiniGPT-4		InternVL3		Qwen2.5VL		Average	
Method	Ci ↓	Cs ↓	Ci ↓	Cs ↓	Ci ↓	Cs ↓	Ci ↓	Cs ↓	Ci ↓	Cs ↓	Ci ↓	Cs ↓
Greedy	14.1	49.2	13.3	48.4	9.9	45.0	7.8	31.6	9.8	40.0	11.0	42.8
Beam	14.2	51.8	14.3	54.6	13.9	48.8	7.6	31.6	8.4	36.0	11.7	44.6
Dola	19.3	61.2	26.2	73.2	13.8	47.8	10.4	41.6	11.0	41.2	16.1	53.0
OPERA	12.8	44.6	14.2	46.4	12.8	44.6	-	-	-	-	-	-
Deco	12.5	46.4	13.5	46.4	9.4	32.2	8.0	33.2	9.4	38.8	10.6	39.4
SAVER	12.8	40.4	13.6	47.8	10.0	32.8	8.3	32.8	8.4	35.6	10.5	37.4
SAKED	11.6	39.6	14.0	42.2	7.7	30.8	7.5	30.4	7.6	32.2	9.7	35.0

Table 2. Hallucination evaluation results on POPE across five models. The performance is the average F1 scores across the three evaluation settings: popular, random, and adversarial.

Method	LLaVA1.5	InstructBLIP	MiniGPT-4	InternVL3	Qwen2.5VL	Average
Greedy	0.8220	0.8000	0.5850	0.9074	0.8136	0.7856
Beam	0.8490	0.8440	0.7030	0.9021	0.8138	0.8224
Dola	0.8320	0.8340	0.7280	0.8657	0.7489	0.8017
Deco	0.8320	0.8492	0.7714	0.9069	0.8136	0.8346
SAVER	0.8489	0.8486	0.7680	0.9063	0.8137	0.8371
SAKED	0.8536	0.8551	0.7639	0.9027	0.8721	0.8495

4. Experiments

4.1. Implementation Details

Evaluation Models and Settings. We evaluate our proposed method and baseline approaches on five representative LVLMs: LLaVA-1.5 (Liu et al., 2023), InstructBLIP (Dai et al., 2023), MiniGPT-4 (Zhu et al., 2023), InternVL3 (Zhu et al., 2025), and Qwen2.5-VL (Bai et al., 2025). Please refer to the Appendix A for the detailed settings of our method.

Baseline Methods. We compare our method with two vanilla decoding strategies (greedy decoding and beam search) as well as four SOTA hallucination mitigation methods, detailed as follows: Dola (Chuang et al., 2023) is specifically designed for alleviating hallucinations in factual tasks for LLMs by reducing shallow semantic influences to improve the factuality of the final layer’s output. OPERA (Huang et al., 2024) is a training-free decoding strategy that mitigates hallucinations in LVLMs by penalizing over-trusted summary tokens in self-attention during beam search and retrospectively reallocating token choices to better incorporate visual information. Deco (Wang et al., 2024a) adaptively chooses relevant layers and integrates their knowledge into the final layer to adjust outputs. SAVER (Li et al., 2026) leverages early-layer, token-level visual attention feedback to dynamically revise LVLM outputs, effectively reducing hallucinations. For all baselines, we either reproduce the methods using the latest model versions or follow the hyperparameter settings recommended

in the officially released code to ensure fair comparisons.

Benchmark and Metrics. We evaluate the effectiveness, generalizability, and language quality of our method across four challenging benchmarks: • **CHAIR**: (Rohrbach et al., 2018) Using the prompt “Please describe the image in detail,” we assess instance- and sentence-level hallucination rates with CHAIRi and CHAIRs. • **POPE**: (Li et al., 2023b) Following the official POPE protocol, we report average F1 scores across three different settings as the primary metric. • **MME** (Fu et al., 2024) is a practical benchmark encompassing a wide range of sub-tasks, including Existence, Count, Position, Color, Poster, Celebrity, Scene, Landmark, Artwork, and OCR, etc. • **AMBER** (Wang et al., 2023) evaluates hallucinations from more diverse perspectives such as attribute, relation, and existence.

4.2. Experiments on CHAIR

Caption Hallucination Assessment with Image Relevance (CHAIR) (Rohrbach et al., 2018) contains 500 images from the MSCOCO2014 validation set. It evaluates caption hallucination at both the instance-level and the sentence-level using the following metrics:

$$\text{CHAIR}_i = \frac{|\{\text{hallucinated instances}\}|}{|\{\text{all mentioned instances}\}|} \quad (13)$$

$$\text{CHAIR}_s = \frac{|\{\text{hallucinated captions}\}|}{|\{\text{all captions}\}|} \quad (14)$$

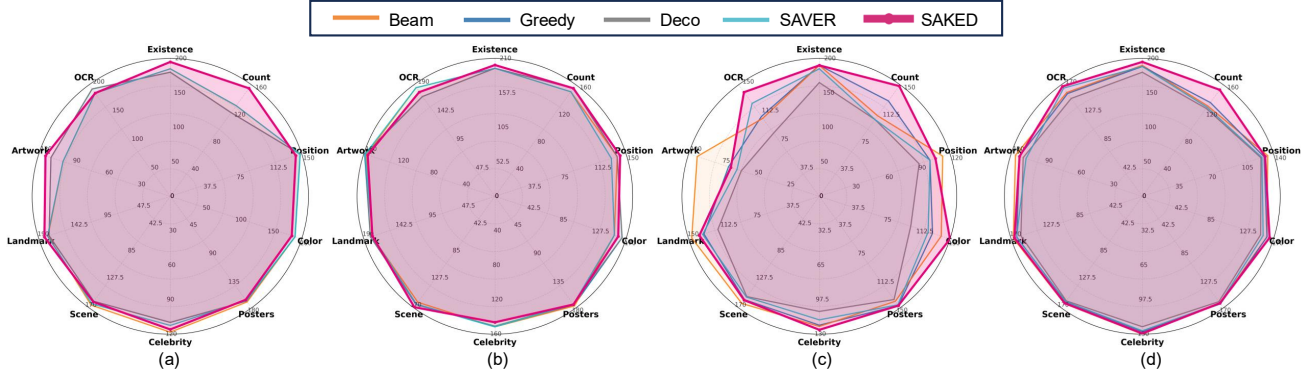


Figure 6. Detailed MME evaluation results on 10 subsets: Existence, Count, Position, Color, Poster, Celebrity, Scene, Landmark, Artwork, and OCR on (a) Qwen2.5VL, (b) InternVL3, (c) LLaVA1.5, and (d) Average results on the three models.

Table 3. Hallucination evaluation results on AMBER. (Hal-Rate: hallucination rate; Cog: cognitive score; Avg. F1 indicates the average F1 scores across the following tasks: Discriminative, Existence, Attribute, State, Number, Action, and Relation.)

Model	Qwen2.5VL				InternVL3				LLaVA1.5				
	Method	CHAIR ↓	Hal-Rate ↓	Cog ↓	Avg. F1 ↑	CHAIR ↓	Hal-Rate ↓	Cog ↓	Avg. F1 ↑	CHAIR ↓	Hal-Rate ↓	Cog ↓	Avg. F1 ↑
Greedy		3.7	16.1	0.7	84.4	3.7	14.5	0.6	72.2	5.5	22.4	2.2	73.7
Beam		3.6	15.6	0.6	84.9	3.2	12.7	0.6	73.3	5.5	21.0	2.1	74.5
Dola		5.1	21.1	1.0	81.8	4.7	15.2	0.7	64.4	7.4	30.1	2.8	78.2
Deco		3.7	16.1	0.7	84.4	3.6	14.5	0.7	72.5	5.8	21.8	2.3	60.8
SAVER		3.5	15.6	0.6	84.7	4.1	16.1	0.6	71.5	6.1	22.5	2.1	68.7
SAKED		3.8	14.4	0.6	86.5	2.7	11.0	0.6	74.1	4.9	20.0	1.9	75.4

Table 1 reports hallucination performance on the CHAIR benchmark across five representative LVLMs, measured by CHAIRi (Ci) and CHAIRs (Cs), where lower values indicate fewer hallucinated objects and sentences. Greedy and Beam decoding exhibit consistently high hallucination rates across models, with average Ci/Cs of 11.0/42.8 and 11.7/44.6 respectively. Language-based method Dola ignores the visual information, thereby significantly degrading performance on various models. Hallucination-aware decoding methods (e.g., OPERA, Deco, SAVER) enhance models’ visual perception and show partial improvements on some models. However, they fail to generalize consistently across architectures. And OPERA cannot be applied to all models due to architectural constraints. In contrast, our method SAKED achieves the lowest hallucination rates on almost all evaluated models, yielding the best average performance with Ci = 9.7 and Cs = 35.0, outperforming all baselines. These results validate that unstable internal knowledge commonly exists in different models, which induce hallucinations. By dynamically leveraging the most stable internal knowledge without additional training, SAKED achieves state-of-the-art hallucination mitigation performance and can be flexibly adapted to different architectures.

4.3. Experiments on POPE

Unlike image captioning, the Polling based Object Probing Evaluation (POPE) (Li et al., 2023b) is a VQA benchmark that contains 500 images from MSCOCO2014, with

six questions paired with each image. POPE evaluates object hallucination by asking binary questions of the form “Is there a <object> in the image?” It includes three <object> settings: random (objects are sampled at random), popular (objects occur frequently), and adversarial (objects are closely related to those present in the image). Table 2 summarizes hallucination mitigation performance on POPE using the average F1 score across the random, popular, and adversarial settings. Prior methods such as Deco and SAVER improve visual perception, yet they remain inferior to our method. In contrast, SAKED yields consistent gains across backbones and achieves the highest average F1 score of 0.8495 among all compared methods. This consistency across diverse LVLM architectures suggests that hallucinations are not solely due to limited visual perception, but are also closely related to unstable knowledge aggregation.

4.4. Experiments on MME

MME (Fu et al., 2024) is a comprehensive evaluation benchmark designed to systematically assess the capabilities of LVLMs in understanding and reasoning over images. MME focuses on perception-oriented and cognition-oriented abilities with “yes/no” question format, covering a wide range of visual tasks such as Existence, Count, Position, Color, Poster, Celebrity, Scene, Landmark, Artwork, and OCR. Detailed results on specific tasks are shown in Figure 6, where our method consistently achieves outstanding evaluation

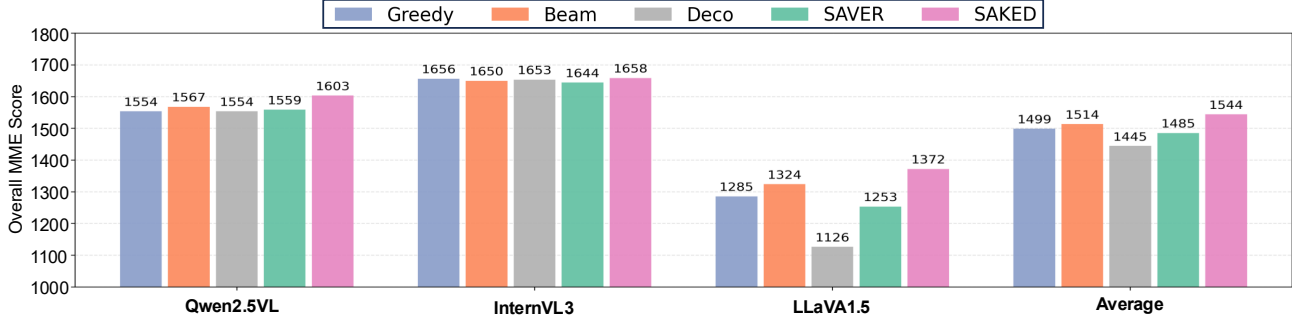


Figure 7. Overall scores on Qwen2.5VL, InternVL3 and, LLaVA1.5 on MME full evaluation set. Higher scores indicate better general capability across perception and reasoning tasks.

Table 4. Ablation study of SAKED on CHAIR. Each row ablates one designed component of the proposed method.

Model	LLaVA1.5		InstructBLIP		InternVL3		Qwen2.5VL		Average	
Method	Ci ↓	Cs ↓	Ci ↓	Cs ↓	Ci ↓	Cs ↓	Ci ↓	Cs ↓	Ci ↓	Cs ↓
w/o CHSS	13.5	44.8	14.1	42.4	8.0	33.0	7.0	32.4	10.7	38.1
w/o CLSS	12.1	41.0	17.5	48.4	8.3	32.4	7.5	32.4	11.4	38.6
w/o CTSS	12.4	42.4	15.1	47.6	7.8	30.2	8.0	34.2	10.8	38.6
w/o SACD	12.0	43.6	15.9	44.8	8.1	31.0	7.5	34.8	10.9	38.6
SAKED	11.0	38.0	14.0	42.2	7.5	30.4	7.6	32.2	10.0	35.7

scores on Qwen2.5VL, InternVL3 and LLaVA1.5 across different tasks. Figure 7 shows the overall scores across these tasks. SAKED consistently achieves the highest performance on all evaluated models in both perception-oriented and cognition-oriented tasks, yielding an average score of 1544, surpassing both the vanilla decoding strategy and previous hallucination mitigation methods.

4.5. Experiments on AMBER

Table 3 reports hallucination evaluation results on the AMBER benchmark across three LVLMs, measured by CHAIR, hallucination rate (Hal-Rate), cognitive score (Cog), and average F1 score over seven fine-grained tasks: Discriminative, Existence, Attribute, State, Number, Action, and Relation. Overall, SAKED demonstrates the most balanced and robust performance, achieving consistent reductions in hallucination-related metrics while maintaining outstanding task accuracy. By explicitly leveraging stability cues during decoding, SAKED effectively suppresses unreliable reasoning paths and achieves outstanding hallucination mitigation performance on both perception- and cognition-oriented metrics.

4.6. Ablation Studies

To evaluate the effectiveness of the proposed components, namely CHSS, CLSS, CTSS, and SACD, we report an ablation study of SAKED on the CHAIR benchmark across four representative LVLMs in Table 4. Removing any component consistently degrades hallucination mitigation performance, which validates the contribution of each module. The full

Table 5. Ablation study on score weights λ_1 , λ_2 , and λ_3 , where λ_1 is fixed to 1.0.

		LLaVA1.5		InstructBLIP		InternVL3		Qwen2.5VL		Average	
λ_2	λ_3	Ci ↓	Cs ↓	Ci ↓	Cs ↓	Ci ↓	Cs ↓	Ci ↓	Cs ↓	Ci ↓	Cs ↓
0.5	1.0	12.7	43.4	14.1	44.8	7.6	30.2	7.9	33.2	10.6	37.9
1.0	0.5	12.0	41.6	17.7	45.6	7.4	28.0	7.7	32.8	11.2	37.0
1.0	1.0	11.6	39.6	14.0	42.2	7.5	30.4	7.6	32.2	10.2	36.1
1.0	2.0	13.0	42.0	14.9	45.0	7.6	30.4	8.2	36.4	10.9	38.5
2.0	1.0	12.3	41.0	14.6	45.4	7.4	29.4	7.6	32.2	10.5	37.0

SAKED framework achieves the best average results across the listed models (Ci=10.0 and Cs=35.7), indicating that cross-head, cross-layer, and cross-token stability modeling provides complementary benefits. In addition, removing SACD consistently worsens performance across all models, which supports its role in enhancing the decoding process. Overall, leveraging stability cues during token generation effectively helps reduce reliance on unstable internal knowledge and mitigates error propagation during decoding.

We further analyze the impact of the score weights λ_1 , λ_2 , and λ_3 . Since KSS is used only for layer selection, the relative contributions of CHSS, CLSS, and CTSS are critical. We fix λ_1 to 1.0 and tune λ_2 and λ_3 in Table 5. The best performance is achieved with $\lambda_2 = 1.0$ and $\lambda_3 = 1.0$, yielding average Ci and Cs of 10.2 and 36.1, respectively. Additional ablations on the contrastive weight α , the token revision weight β , and the candidate layer set L_c are provided in Appendix B.3.

5. Conclusion

In this paper, we present Stability-Aware Knowledge Enhanced Decoding (SAKED), a training-free and plug-and-play decoding strategy for mitigating hallucinations in LVLMs. Through extensive analyses, we show that hallucinations are closely related to internal knowledge instability along three dimensions: visual information drift across attention heads, knowledge fluctuations across layers, and visual focus distraction between adjacent tokens. Building on these findings, we propose a Knowledge Stability Score (KSS) that quantifies layer-wise knowledge stability

for each generated token by integrating CHSS, CLSS, and CTSS. We then use KSS to dynamically identify the most “stable” and most “unstable” layers and contrast their logits to further improve decoding faithfulness. Extensive experiments show that SAKED consistently enhances faithfulness across a wide range of tasks and benchmarks. SAKED requires neither external information nor model fine-tuning and can be readily adapted to different architectures. Overall, our study advances the understanding of hallucination mechanisms in LVLMs, and SAKED provides a practical step toward safer and more reliable multimodal generation.

Impact Statement

This work tackles a key barrier to deploying LVLMs in real-world settings: hallucinated content that undermines trust and safety. We present a training-free, plug-and-play decoding strategy that mitigates hallucinations without requiring additional data, external knowledge sources, or any model fine-tuning. Beyond proposing a practical remedy, we provide a systematic analysis linking hallucinated outputs to internal knowledge instability. Guided by these insights, our method significantly improves generation faithfulness and strengthens the reliability of LVLM outputs, supporting safer and more trustworthy use across diverse applications. More broadly, our findings offer a principled lens for diagnosing hallucinations and may catalyze follow-up research toward more general, widely deployable approaches for improving LVLM reliability.

References

Alayrac, J.-B., Donahue, J., Luc, P., Miech, A., Barr, I., Hasson, Y., Lenc, K., Mensch, A., Millican, K., Reynolds, M., et al. Flamingo: a visual language model for few-shot learning. *Advances in neural information processing systems*, 35:23716–23736, 2022.

Awadalla, A., Gao, I., Gardner, J., Hessel, J., Hanafy, Y., Zhu, W., Marathe, K., Bitton, Y., Gadre, S., Sagawa, S., et al. Openflamingo: An open-source framework for training large autoregressive vision-language models. *arXiv preprint arXiv:2308.01390*, 2023.

Bai, S., Chen, K., Liu, X., Wang, J., Ge, W., Song, S., Dang, K., Wang, P., Wang, S., Tang, J., et al. Qwen2. 5-vl technical report. *arXiv preprint arXiv:2502.13923*, 2025.

Chen, K., Zhang, Z., Zeng, W., Zhang, R., Zhu, F., and Zhao, R. Shikra: Unleashing multimodal llm’s referential dialogue magic. *arXiv preprint arXiv:2306.15195*, 2023.

Chen, S., Xiong, M., Liu, J., Wu, Z., Xiao, T., Gao, S., and He, J. In-context sharpness as alerts: An inner representation perspective for hallucination mitigation. *arXiv preprint arXiv:2403.01548*, 2024a.

Chen, Z., Zhao, Z., Luo, H., Yao, H., Li, B., and Zhou, J. Halc: Object hallucination reduction via adaptive focal-contrast decoding. *arXiv preprint arXiv:2403.00425*, 2024b.

Chuang, Y.-S., Xie, Y., Luo, H., Kim, Y., Glass, J., and He, P. Dola: Decoding by contrasting layers improves factuality in large language models. *arXiv preprint arXiv:2309.03883*, 2023.

Dai, W., Li, J., Li, D., Tiong, A. M. H., Zhao, J., Wang, W., Li, B., Fung, P., and Hoi, S. Instructblip: Towards general-purpose vision-language models with instruction tuning, 2023.

Fang, H., Zhou, C., Kong, J., Gao, K., Chen, B., Liang, T., Ma, G., and Xia, S.-T. Grounding language with vision: A conditional mutual information calibrated decoding strategy for reducing hallucinations in lvms. *arXiv preprint arXiv:2505.19678*, 2025a.

Fang, Y., Yang, Z., Chen, Z., Zhao, Z., and Zhou, J. Enhancing vision-language model reliability with uncertainty-guided dropout decoding. In *The Thirty-ninth Annual Conference on Neural Information Processing Systems*, 2025b.

Favero, A., Zancato, L., Trager, M., Choudhary, S., Perera, P., Achille, A., Swaminathan, A., and Soatto, S. Multi-modal hallucination control by visual information grounding. In *Proceedings of the IEEE/CVF Conference on Computer Vision and Pattern Recognition*, pp. 14303–14312, 2024.

Fu, C., Chen, P., Shen, Y., Qin, Y., Zhang, M., Lin, X., Yang, J., Zheng, X., Li, K., Sun, X., Wu, Y., and Ji, R. Mme: A comprehensive evaluation benchmark for multimodal large language models, 2024. URL <https://arxiv.org/abs/2306.13394>.

Gong, X., Ming, T., Wang, X., and Wei, Z. Damro: Dive into the attention mechanism of lvlm to reduce object hallucination. *arXiv preprint arXiv:2410.04514*, 2024.

Google DeepMind. Introducing gemini 3. <https://blog.google/products/gemini/gemini-3/>, 2025. Accessed: 2025-12.

He, L., Chen, Z., Shi, Z., Yu, T., Shao, J., and Sheng, L. Systematic reward gap optimization for mitigating vlm hallucinations. In *The Thirty-ninth Annual Conference on Neural Information Processing Systems*.

Heiman, A., Zhang, X., Chen, E., Kim, S. E., and Rajpurkar, P. Factchexcker: Mitigating measurement hallucinations in chest x-ray report generation models. In *Proceedings of the Computer Vision and Pattern Recognition Conference*, pp. 30787–30796, 2025.

Huang, Q., Dong, X., Zhang, P., Wang, B., He, C., Wang, J., Lin, D., Zhang, W., and Yu, N. Opera: Alleviating hallucination in multi-modal large language models via over-trust penalty and retrospection-allocation. In *Proceedings of the IEEE/CVF Conference on Computer Vision and Pattern Recognition*, pp. 13418–13427, 2024.

Jiang, C., Xu, H., Dong, M., Chen, J., Ye, W., Yan, M., Ye, Q., Zhang, J., Huang, F., and Zhang, S. Hallucination augmented contrastive learning for multimodal large language model. In *Proceedings of the IEEE/CVF Conference on Computer Vision and Pattern Recognition*, pp. 27036–27046, 2024.

Jing, L. and Du, X. Fgaif: Aligning large vision-language models with fine-grained ai feedback. *arXiv preprint arXiv:2404.05046*, 2024.

Kalai, A. T., Nachum, O., Vempala, S. S., and Zhang, E. Why language models hallucinate. *arXiv preprint arXiv:2509.04664*, 2025.

Kang, S., Kim, J., Kim, J., and Hwang, S. J. See what you are told: Visual attention sink in large multimodal models. *arXiv preprint arXiv:2503.03321*, 2025.

Kong, C., Luo, A., Bao, P., Yu, Y., Li, H., Zheng, Z., Wang, S., and Kot, A. C. Moe-ffd: Mixture of experts for generalized and parameter-efficient face forgery detection. *IEEE Transactions on Dependable and Secure Computing*, 2025.

Leng, S., Zhang, H., Chen, G., Li, X., Lu, S., Miao, C., and Bing, L. Mitigating object hallucinations in large vision-language models through visual contrastive decoding. In *Proceedings of the IEEE/CVF Conference on Computer Vision and Pattern Recognition*, pp. 13872–13882, 2024.

Li, J., Li, D., Savarese, S., and Hoi, S. Blip-2: Bootstrapping language-image pre-training with frozen image encoders and large language models. In *International conference on machine learning*, pp. 19730–19742. PMLR, 2023a.

Li, Y., Du, Y., Zhou, K., Wang, J., Zhao, W. X., and Wen, J.-R. Evaluating object hallucination in large vision-language models. *arXiv preprint arXiv:2305.10355*, 2023b.

Li, Z., Shi, H., Gao, Y., Liu, D., Wang, Z., Chen, Y., Liu, T., Zhao, L., Wang, H., and Metaxas, D. N. The hidden life of tokens: Reducing hallucination of large vision-language models via visual information steering. *arXiv preprint arXiv:2502.03628*, 2025.

Li, Z., Kong, C., Yu, Y., Wu, Q., Jiang, X., Cheung, N.-M., Wen, B., Kot, A., and Jiang, X. Saver: Mitigating hallucinations in large vision-language models via style-aware visual early revision. *The Association for the Advancement of Artificial Intelligence (AAAI)*, 2026.

Liu, H., Li, C., Wu, Q., and Lee, Y. J. Visual instruction tuning. *Advances in neural information processing systems*, 36:34892–34916, 2023.

Liu, S., Zheng, K., and Chen, W. Paying more attention to image: A training-free method for alleviating hallucination in llmms. In *European Conference on Computer Vision*, pp. 125–140. Springer, 2024.

Lv, Q., Wang, J., Chen, H., Li, B., Zhang, Y., and Wu, F. Coarse-to-fine highlighting: Reducing knowledge hallucination in large language models. *arXiv preprint arXiv:2410.15116*, 2024.

OpenAI. Gpt-4 technical report. <https://openai.com/research/gpt-4>, 2023. Accessed: 2024-10-18.

OpenAI. Introducing gpt-5. <https://openai.com/index/introducing-gpt-5/>, 2025. Accessed: 2025-12-20.

Park, S., Du, X., Yeh, M.-H., Wang, H., and Li, Y. Steer llm latents for hallucination detection. *arXiv preprint arXiv:2503.01917*, 2025a.

Park, W., Kim, W., Kim, J., and Do, J. Second: Mitigating perceptual hallucination in vision-language models via selective and contrastive decoding. *arXiv preprint arXiv:2506.08391*, 2025b.

Rohrbach, A., Hendricks, L. A., Burns, K., Darrell, T., and Saenko, K. Object hallucination in image captioning. *arXiv preprint arXiv:1809.02156*, 2018.

Sarkar, P., Ebrahimi, S., Etemad, A., Beirami, A., Arik, S. Ö., and Pfister, T. Mitigating object hallucination in mllms via data-augmented phrase-level alignment. *International Conference on Learning Representations*, 2025.

Tan, C., Qu, Y., Li, X., Zhang, H., Cui, S., Chen, C., and Gao, L. Wisdom is knowing what not to say: Hallucination-free llms unlearning via attention shifting. *arXiv preprint arXiv:2510.17210*, 2025.

Wang, C., Chen, X., Zhang, N., Tian, B., Xu, H., Deng, S., and Chen, H. Mllm can see? dynamic correction decoding for hallucination mitigation. *arXiv preprint arXiv:2410.11779*, 2024a.

Wang, J., Wang, Y., Xu, G., Zhang, J., Gu, Y., Jia, H., Wang, J., Xu, H., Yan, M., Zhang, J., et al. Amber: An llm-free multi-dimensional benchmark for mllms hallucination evaluation. *arXiv preprint arXiv:2311.07397*, 2023.

Wang, L., He, J., Li, S., Liu, N., and Lim, E.-P. Mitigating fine-grained hallucination by fine-tuning large vision-language models with caption rewrites. In *International*

Conference on Multimedia Modeling, pp. 32–45. Springer, 2024b.

Wang, S., Zhang, Y., Zhu, Y., Liu, E., Li, J., Liu, Y., and Ji, X. Shift: Smoothing hallucinations by information flow tuning for multimodal large language models. In *Proceedings of the IEEE/CVF International Conference on Computer Vision*, pp. 3639–3649, 2025a.

Wang, W., Ding, Z., Gu, J., Cao, R., Meinel, C., de Melo, G., and Yang, H. Image tokens matter: Mitigating hallucination in discrete tokenizer-based large vision-language models via latent editing. *arXiv preprint arXiv:2505.21547*, 2025b.

Wu, M., Ji, J., Huang, O., Li, J., Wu, Y., Sun, X., and Ji, R. Evaluating and analyzing relationship hallucinations in large vision-language models. *arXiv preprint arXiv:2406.16449*, 2024.

Xia, S., Ding, M., Kong, C., Yang, W., and Jiang, X. Provable robustness in multimodal large language models via feature space smoothing. *arXiv preprint arXiv:2601.16200*, 2026.

Xu, H., Zhu, Z., Pan, L., Wang, Z., Zhu, S., Ma, D., Cao, R., Chen, L., and Yu, K. Reducing tool hallucination via reliability alignment. *arXiv preprint arXiv:2412.04141*, 2024.

Yang, Z., Luo, X., Han, D., Xu, Y., and Li, D. Mitigating hallucinations in large vision-language models via dpo: On-policy data hold the key. In *Proceedings of the Computer Vision and Pattern Recognition Conference*, pp. 10610–10620, 2025.

Yin, S., Fu, C., Zhao, S., Li, K., Sun, X., Xu, T., and Chen, E. A survey on multimodal large language models. *National Science Review*, 11(12), 2024.

Zhang, J., Wang, T., Zhang, H., Lu, P., and Zheng, F. Reflective instruction tuning: Mitigating hallucinations in large vision-language models. In *European Conference on Computer Vision*, pp. 196–213. Springer, 2024.

Zhang, M., Press, O., Merrill, W., Liu, A., and Smith, N. A. How language model hallucinations can snowball. *arXiv preprint arXiv:2305.13534*, 2023.

Zhao, L., Deng, Y., Zhang, W., and Gu, Q. Mitigating object hallucination in large vision-language models via image-grounded guidance. *arXiv preprint arXiv:2402.08680*, 2024a.

Zhao, Z., Tang, J., Wu, B., Lin, C., Wei, S., Liu, H., Tan, X., Zhang, Z., Huang, C., and Xie, Y. Harmonizing visual text comprehension and generation. *arXiv preprint arXiv:2407.16364*, 2024b.

Zhou, Y., Cui, C., Yoon, J., Zhang, L., Deng, Z., Finn, C., Bansal, M., and Yao, H. Analyzing and mitigating object hallucination in large vision-language models. *arXiv preprint arXiv:2310.00754*, 2023.

Zhu, C., Liu, Y., Zhang, H., Wang, A., Chen, G., Wang, L., Luo, W., Zhang, K., et al. Alleviating hallucinations in large language models through multi-model contrastive decoding and dynamic hallucination detection. In *The Thirty-ninth Annual Conference on Neural Information Processing Systems*.

Zhu, D., Chen, J., Shen, X., Li, X., and Elhoseiny, M. Minigpt-4: Enhancing vision-language understanding with advanced large language models. *arXiv preprint arXiv:2304.10592*, 2023.

Zhu, J., Wang, W., Chen, Z., Liu, Z., Ye, S., Gu, L., Tian, H., Duan, Y., Su, W., Shao, J., et al. Internvl3: Exploring advanced training and test-time recipes for open-source multimodal models. *arXiv preprint arXiv:2504.10479*, 2025.

Zou, X., Wang, Y., Yan, Y., Lyu, Y., Zheng, K., Huang, S., Chen, J., Jiang, P., Liu, J., Tang, C., et al. Look twice before you answer: Memory-space visual retracing for hallucination mitigation in multimodal large language models. *arXiv preprint arXiv:2410.03577*, 2024.

Table 6. Results of different maximum generation lengths on LLaVA-1.5 and Qwen2.5-VL. Our method consistently achieves lower Ci and Cs than vanilla decoding across all token budgets, with larger improvement at longer generation lengths.

Model	LLaVA1.5						Qwen2.5VL							
	Max. tokens		64		256		512		64		256		512	
Method	Ci ↓	Cs ↓	Ci ↓	Cs ↓	Ci ↓	Cs ↓	Ci ↓	Cs ↓	Ci ↓	Cs ↓	Ci ↓	Cs ↓	Ci ↓	Cs ↓
Vanilla	7.3	22.8	14.4	48.8	14.1	49.2	6.3	15.0	8.9	36.6	9.8	40.0		
+SAKED	6.9	19.8	12.8	43.0	11.6	39.6	4.6	10.0	7.5	30.4	7.6	32.2		

A. Experiment Setup

A.1. Additional Implementation Details

All experiments are conducted using deterministic decoding without sampling. We fix the decoding parameters, including top- k , top- p , and temperature to 1 for all datasets. The maximum generation length is set to 512 tokens for CHAIR, 64 tokens for AMBER, and 10 tokens for POPE and MME, respectively. The beam search variant in our experiment essentially adopts a beam width of 5 while maintaining the others. Unless otherwise specified, all evaluated models are based on 7B-scale language backbones.

A.2. Hardware Setup

We run our benchmark and decoding method comparison experiments using one NVIDIA GPU with 48 GB of memory.

B. Additional Experimental Results

B.1. Results of Different Maximum Token Numbers

Table 6 reports the results of different maximum generation lengths on LLaVA-1.5 and Qwen2.5-VL. Results are shown for maximum token limits of 64, 256, and 512, evaluated using two metrics, Ci and Cs from the CHAIR benchmark. We compare vanilla greedy decoding with our proposed method SAKED. Across all token budgets and both models, our method consistently outperforms greedy decoding, yielding lower Ci and Cs scores. The performance gain enhances as the maximum token limit increases, indicating that our approach scales more favorably with longer generations and better controls error accumulation in extended outputs.

B.2. Language Quality Evaluations

Table 7 reports a comprehensive comparison of language quality among hallucination mitigation methods on three representative multimodal large language models: LLaVA-1.5, InternVL3, and InstructBLIP. We evaluate generation quality using BLEU-1/2/3/4, METEOR, and ROUGE-L, which jointly measure lexical overlap, n-gram consistency, and semantic alignment with ground-truth responses. Best and second-best results are highlighted in bold and underlined, respectively.

On LLaVA-1.5, SAKED consistently outperforms all baselines across every metric, achieving the highest BLEU scores at all n-gram levels as well as the best METEOR and ROUGE-L results. This indicates that SAKED not only improves surface-level fluency but also enhances semantic fidelity while mitigating hallucinations. Dola and Deco provide moderate improvements over SAVER, but remain consistently below SAKED. For InternVL3, Deco achieves the strongest overall performance, obtaining the best scores across all evaluation metrics. While SAKED does not surpass Deco on this model, it remains competitive and outperforms Dola on all metrics. On InstructBLIP, SAKED again demonstrates superior performance, yielding the best BLEU-1/2, METEOR, and ROUGE-L scores, while achieving comparable BLEU-3/4 results to Deco and SAVER. These results highlight SAKED’s robustness in preserving both lexical accuracy and semantic consistency.

When averaging results across all three models, SAKED achieves the highest overall BLEU-1, BLEU-2, METEOR, and ROUGE-L scores, and remains highly competitive on BLEU-3 and BLEU-4. This consistent improvement across diverse architectures suggests that SAKED provides a favorable balance between hallucination mitigation and language quality, avoiding the degradation in fluency or informativeness observed in some prior methods.

Table 7. Language quality comparison of hallucination mitigation methods on LLaVA-1.5, InternVL3, and InstructBLIP. Results are reported in BLEU-1/2/3/4, METEOR, and ROUGE-L.

Model	Method	BLEU-1 ↑	BLEU-2 ↑	BLEU-3 ↑	BLEU-4 ↑	METEOR ↑	ROUGEL ↑
LLaVA-1.5	Dola	<u>18.9</u>	<u>11.0</u>	6.3	3.9	<u>31.8</u>	<u>16.0</u>
	Deco	17.0	<u>11.0</u>	<u>6.6</u>	<u>4.1</u>	29.8	15.5
	SAVER	16.3	10.2	6.0	3.7	29.0	14.8
	SAKED	19.2	12.0	7.1	4.4	32.5	17.1
InternVL3	Dola	11.5	7.0	3.7	2.2	22.8	10.3
	Deco	14.2	9.1	5.3	3.3	26.5	12.7
	SAVER	<u>13.9</u>	<u>8.6</u>	<u>4.9</u>	<u>3.0</u>	<u>26.4</u>	<u>12.3</u>
	SAKED	12.4	7.8	4.3	2.6	24.0	11.1
InstructBLIP	Dola	14.0	8.1	4.6	2.8	26.7	12.1
	Deco	<u>15.9</u>	<u>10.6</u>	6.6	4.2	<u>29.4</u>	<u>14.7</u>
	SAVER	15.0	10.3	6.4	<u>4.1</u>	28.2	14.3
	SAKED	16.6	10.7	<u>6.5</u>	<u>4.1</u>	30.4	14.9
Average	Dola	14.8	8.7	4.9	3.0	27.1	12.8
	Deco	<u>15.7</u>	10.2	6.2	3.9	<u>28.6</u>	<u>14.3</u>
	SAVER	15.1	<u>9.7</u>	5.8	3.6	27.9	13.8
	SAKED	16.1	10.2	<u>6.0</u>	<u>3.7</u>	29.0	14.4

B.3. Additional Ablation Studies

We conduct extensive ablation studies on three key hyper-parameters, α , β , and L_c , across five representative LVLMs evaluated on the CHAIR benchmark. Following previous works (Chuang et al., 2023; Huang et al., 2024; Li et al., 2026), we set varying parameter values for different models.

B.3.1. EFFECT OF THE WEIGHT α IN SCAD

Table 8 summarizes the ablation results for the SCAD weighting factor α , where highlighted cells correspond to our selected hyper-parameters. For LLaVA-1.5, increasing α consistently decreases the Ci metric, with the lowest value observed at $\alpha = 0.5$, while Cs achieves its minimum at $\alpha = 0.4$, suggesting that slightly larger α values are more beneficial for reducing instance-level hallucinations. InstructBLIP exhibits a similar pattern, where Ci is minimized at $\alpha = 0.4$ and Cs at $\alpha = 0.5$, indicating a trade-off between the two metrics. InternVL3 demonstrates relatively stable Ci performance across different α values, whereas Cs reaches its optimal value at $\alpha = 0.1$, implying that smaller α values are more effective in mitigating sentence-level hallucinations for this model. For Qwen2.5-VL, Ci is minimized at $\alpha = 0.4$, while Cs attains its lowest value at $\alpha = 0.3$, reflecting balanced sensitivity to α . MiniGPT-4 achieves its best Cs performance at $\alpha = 0.5$.

Overall, these findings suggest that moderate values of α generally provide a favorable balance between Ci and Cs across diverse architectures, while also highlighting the importance of model-specific tuning to further improve consistency performance.

B.3.2. EFFECT OF FINAL OUTPUT REVISION WEIGHT β

Following the CHAIR benchmark, we investigate the impact of the token revision weight β on both Ci and Cs as shown in Table 9.

Overall, the results indicate that β plays an important role in balancing instance-level and sentence-level hallucination. For LLaVA1.5, both Ci and Cs are minimized at $\beta = 0.8$, suggesting that a moderate β is effective in reducing hallucinations at both levels. InstructBLIP exhibits lower Ci and Cs at smaller β values, while larger β leads to increased hallucination, indicating higher sensitivity to this parameter. For InternVL3, the lowest Ci and Cs are achieved at $\beta = 0.4$, and performance remains relatively stable as β increases, demonstrating robustness to different β settings. Qwen2.5VL achieves the lowest Ci at $\beta = 1.0$, while Cs is minimized at $\beta = 0.8$ and $\beta = 1.2$, reflecting a trade-off between instance-level and sentence-level hallucination. MiniGPT-4 shows the best instance-level consistency at $\beta = 1.0$, whereas sentence-level hallucination is minimized at $\beta = 0.4$.

Table 8. Ci and Cs results under different α .

α	LLaVA1.5		InstructBLIP		InternVL3		Qwen2.5VL		MiniGPT-4	
	Ci \downarrow	Cs \downarrow								
0.1	12.4	41.4	14.2	47.0	7.6	30.2	7.3	32.6	7.7	30.8
0.2	12.5	42.8	14.2	44.6	7.6	30.4	7.8	36.8	11.6	35.2
0.3	12.5	41.8	14.2	45.6	8.1	32.4	7.6	32.2	9.4	33.4
0.4	11.6	39.6	13.5	43.2	8.1	33.4	7.1	32.4	9.6	31.0
0.5	11.2	39.8	13.6	42.8	7.5	30.4	7.6	35.6	9.0	30.2

 Table 9. Ci and Cs results under different β .

β	LLaVA1.5		InstructBLIP		InternVL3		Qwen2.5VL		MiniGPT-4	
	Ci \downarrow	Cs \downarrow								
0.4	12.9	43.0	13.6	42.8	7.5	30.4	8.7	38.6	9.6	31.0
0.6	12.8	43.0	14.1	45.8	9.3	32.4	7.9	37.2	11.0	35.4
0.8	11.6	39.6	14.8	46.8	7.9	30.8	7.6	32.2	9.8	34.2
1.0	14.4	43.6	17.9	46.4	8.6	32.0	7.4	32.6	8.8	36.6
1.2	12.7	41.8	17.4	46.0	8.0	32.4	8.8	32.2	9.5	37.8

In summary, these results suggest that moderate β values provide a favorable balance between instance-level and sentence-level hallucination across different models, while extreme settings may amplify hallucinations. This demonstrates that the proposed method is effective and robust under a wide range of β values when evaluated with CHAIR.

B.3.3. EFFECT OF DIFFERENT CANDIDATE LAYERS L_c

Due to the variance of model architectures, we select different candidate layers L_c for different models. Table 10 shows that the optimal candidate layer range L_c is model dependent, indicating that the most reliable stability contrast does not occur at a fixed depth across LVLM backbones. For LLaVA1.5, performance improves as L_c shifts deeper, with the best results at 26-30 (Ci=11.6, Cs=39.6), suggesting that stability cues most useful for suppressing hallucinations emerge in late layers. InstructBLIP achieves its best performance in a mid-late range, 22-26 (13.6, 42.8), while both earlier and later ranges degrade results. In contrast, InternVL and Qwen2.5VL favor earlier mid ranges, namely 18-22 (9.6, 31.0) and 16-20 (7.2, 29.6), and their Cs increases noticeably when L_c moves deeper, which is consistent with the hypothesis that later layers can amplify unstable knowledge aggregation or language priors, weakening faithfulness. MiniGPT-4 exhibits a mild tradeoff, where 16-20 yields the lowest Ci but 18-22 yields the lowest Cs, suggesting that instance-level and sentence-level hallucination sensitivity can peak at slightly different depths.

Overall, these results highlight that constraining L_c to an appropriate mid or late block is important for reliably selecting l^+ and l^- , and they motivate choosing L_c in a backbone-aware manner rather than adopting a universal default.

B.4. Visualization Results

We present qualitative examples comparing our method with the baseline greedy decoding strategy and the hallucination mitigation approach Deco. Our method significantly mitigates hallucinations by dynamically refining the decoding process using layer-wise stable knowledge while maintaining high-level quality. Figures 8, 9, 10, and 11 show representative results on LLaVA-1.5, InstructBLIP, Qwen2.5VL, and InternVL3, respectively.

C. Limitations and Future Work

In the early stages of generation, token predictions are typically more stable, which reduces the extent to which temporal dependencies manifest in short sequences. As a result, CTSS has limited impact on short responses because it captures visual focus distraction between neighboring tokens, a signal that becomes more informative as temporal effects accumulate.

Table 10. Ci and Cs results with different L_c .

L_c	LLaVA1.5		InstructBLIP		InternVL		L_c	Qwen2.5VL		MiniGPT-4	
	Ci ↓	Cs ↓	Ci ↓	Cs ↓	Ci ↓	Cs ↓		Ci ↓	Cs ↓	Ci ↓	Cs ↓
18-22	14.7	45.4	14.9	48.6	9.6	31.0	16-20	7.2	29.6	7.3	33.8
20-24	17.6	46.2	15.2	48.8	10.1	32.8	18-22	7.5	30.4	7.6	32.2
22-26	13.9	42.8	13.6	42.8	11.0	31.4	20-24	7.6	30.2	8.1	35.4
24-28	12.8	41.2	13.7	47.2	9.3	37.8	22-26	8.1	32.4	9.0	38.6
26-30	11.6	39.6	14.2	46.6	10.3	35.1	24-28	7.5	31.4	9.6	41.8

Nevertheless, KSS also incorporates CHSS and CLSS, which exploit stable visual activation and layer-wise semantic cues to improve decoding even at early stages. As the sequence length increases, temporal dependencies accumulate, and SAKED remains effective at mitigating hallucinations in longer generations.

For future work, we will investigate more flexible ways to leverage CHSS, CLSS, and CTSS throughout the generation process. For example, these scores can be integrated into decoding with adaptive weighting that varies across generation stages, prediction confidence, or sequence length. Beyond inference time usage, CHSS, CLSS, and CTSS may also serve as auxiliary supervision signals during training, encouraging models to explicitly suppress behaviors that are prone to hallucination.

Prompt:
Describe this image in detail.



LLaVA-1.5-7b (Greedy) :

The image features a man wearing a striped shirt and a tie, sitting in a room with his arms crossed. He appears to be relaxed and comfortable in his surroundings. **The room has a dining table in the background, and a chair is placed nearby. There are two other people in the scene, one standing in the background and another person partially visible on the right side of the image. The room also contains a couch and a handbag placed on the floor.**

LLaVA-1.5-7b (Deco) :

The image features a man wearing a striped shirt and a tie, sitting in a room with his arms crossed. He appears to be relaxed and comfortable in his surroundings. **The room has a dining table in the background, and a chair is placed nearby. There are two other people in the scene, one standing in the background and another person partially visible on the right side of the image. The room also contains a couch and a handbag placed on the floor.**

LLaVA-1.5-7b (SAKED) :

The image depicts a businessman wearing a tie and shirt, leaning against a wall with his arms crossed. He appears to be casually dressed, possibly in a casual office setting or during a break from work. The businessman appears to be relaxed and comfortable in his environment.

LLaVA-1.5-7b (Greedy) :

The image features a man and a woman sitting at a dining table in a kitchen. They are both smiling and enjoying their time together. The table is set with various items, including **a wine glass, a cup, a bowl, and a spoon**. In the background, there is an oven and **a sink**, indicating that the kitchen is well-equipped for cooking and cleaning. The scene also includes a few bottles placed around the kitchen, possibly containing beverages or condiments.

LLaVA-1.5-7b (Deco) :

The image depicts two people, a man and a woman, sitting at a table in a kitchen. They appear to be smiling and enjoying themselves as they engage in conversation. The table is filled with various items such as bottles, **cups**, and utensils like knives and **spoons**. There are several bottles placed on the table, some closer to the man and others nearer to the woman. Cups can be found both near the bottles and on the table itself. The knives and **spoons** are positioned near the bottles, likely ready for use during meal preparation or consumption. The kitchen itself is equipped with an oven, which is located towards the left side of the room. The overall atmosphere of the scene is one of warmth and camaraderie between the two people.

LLaVA-1.5-7b (SAKED) :

The image depicts two people sitting at a table in a kitchen, engaged in conversation. Both individuals are smiling, creating a warm atmosphere. They appear to be enjoying their time together. The kitchen features a stove top oven positioned towards the left side of the room, and an oven located towards the right side. There are several bottles placed around the kitchen area, some closer to the left side of the room and others nearer to the right side. Additionally, there are two knives visible on the right side of the room, likely used for meal preparation.

Prompt:
Describe this image in detail.



LLaVA-1.5-7b (Greedy) :

The image captures a baseball game in progress, with a player standing on the field holding a baseball bat. The player is wearing a **baseball glove**, ready to play. There are several other people in the scene, some of them possibly teammates or opponents. **In the background, a baseball glove can be seen lying on the ground, and a sports ball is visible in the air.** The scene is set on a baseball field, with the players actively participating in the game.

LLaVA-1.5-7b (Deco) :

The image depicts a baseball game in progress on a field. There are several players on the field, some of them wearing baseball gloves. One player is prominently holding a bat, ready to swing at the incoming ball. **Another player can be seen wearing a baseball glove, ready to catch the ball. There are also two baseball gloves visible in the scene, one near the center of the field and another towards the right side.** The players are spread out across the field, some positioned closer to the center while others are positioned towards the edges of the field.

LLaVA-1.5-7b (SAKED) :

The image depicts a baseball game taking place on a field. There are several players on the field, with one player prominently standing near home plate wearing a baseball uniform with the number twenty-five on it. Another player can be seen holding a bat, ready to swing at an incoming pitch. Other players are scattered around the field, some positioned near bases while others stand further away from them. Overall, it's a dynamic scene capturing the essence of a baseball game.

Prompt:
Describe this image in detail.



Figure 8. Qualitative visualization results on LLaVA-1.5 using different decoding methods, with hallucinated content highlighted in red.

InstructBLIP-7b (Greedy) :

Prompt:

Describe this image in detail.



InstructBLIP-7b (Deco) :

The image depicts a bedroom scene where two cats are lying on two pillows placed on a bed. The two cats are positioned side by side, one cat on each pillow, and they appear to be enjoying their time together. The bed itself is covered with pillows, with one in the center and others positioned on either side of the bed. **There are several books in the room, with one book placed near the center of the room and others positioned near the bed.** A laptop computer is also present in the room, positioned near the center of the room.

InstructBLIP-7b (SAKED) :

The image depicts two cats lying on a bed together, one on each side of the bed pillows. They are resting comfortably on the bed, possibly enjoying each other's company or simply enjoying the warmth of the bed. There are several pillows scattered around the bed, including one near each cat's head and others positioned near the foot of the bed. Additionally, there is a laptop placed on the bed near one of the cats, possibly indicating that they are enjoying some downtime together while using the laptop.

InstructBLIP-7b (Greedy) :

The image features a cozy bedroom with a large bed in the center of the room. The bed is adorned with a canopy and a rug, adding a touch of elegance to the space. The room also features a dining table with chairs, a chair, and a couch. There are multiple chairs placed throughout the room, including one near the bed and another near the dining table. **A potted plant can be seen on the right side of the room, adding a touch of nature to the space.** The room is well-decorated and inviting, making it a comfortable and cozy place to relax.

InstructBLIP-7b (Deco) :

The image depicts a room with a bedroom in it. The room is decorated with stripes on the walls and ceiling, and the bedroom itself is furnished with a bed, a chair, and a table. There are several chairs scattered around the room, including one in front of the bed and others positioned near the table. **A TV is also present in the room, positioned near one of the chairs.** The room has a cozy and inviting atmosphere, with a fireplace and a chair next to it. The overall design of the room evokes a Victorian style, with a mix of Victorian and modern elements blending together.

InstructBLIP-7b (SAKED) :

The image depicts a room with a bedroom area and a living room area combined into one space. The bedroom area features a bed with a headboard and a bedside table next to it. There are two chairs placed near the bedside table, one on either side of it. Additionally, there are two tables in the room, one near the bedside table and another near the opposite side of the room. The living room area is decorated with a rug and a chair placed near it. There are two additional chairs placed near the rug, one on either side of it. There are also two additional tables in the room, one near the chair near the rug and another near the opposite side of the room. The room is decorated with a fireplace, which adds warmth and ambiance to the space.

Prompt:
Describe this image in detail.



InstructBLIP-7b (Greedy) :

The image features two young girls sitting on a couch, each with their feet on the floor. They are holding Nintendo Wii controllers, which they are using to play a game. The girls are sitting close to each other, with their feet positioned in front of the couch. The couch is placed in the center of the room, **with a chair and a cup placed nearby. The room appears to be a living space, with a TV visible in the background.** The girls are engrossed in their game, enjoying their time together.

LLaVA-1.5-7b (Deco) :

The image depicts two girls, one in front and one behind, sitting on a couch together. They are both in their bare feet, with one girl in front and one behind. The girls are holding controllers, likely for video games, and are enjoying themselves while playing together. The couch is positioned in front of a **TV, which is located to the left side of the image. There are several objects visible in the room, including a chair, a cup, and a book.** The room appears to be a living room or a living space where the girls are spending time together playing games.

LLaVA-1.5-7b (SAKED) :

The image depicts two young girls sitting on a couch together, each holding a controller for a video game console. They are both wearing shoes, but their feet are visible as they sit on the couch. The girls are positioned close to each other, with one girl sitting on the left side of the couch and the other girl sitting on the right side of the couch. Both girls are enjoying their gameplay together, engrossed in their respective controllers.

Figure 9. Qualitative visualization results on InstructBLIP using different decoding methods, with hallucinated content highlighted in red.

Qwen2.5-VL (Greedy) :

...The motorcycle appears to be a cruiser-style bike, featuring a large front headlight, a prominent engine with exposed pipes, and a rugged design that suggests it is built for both comfort and performance. The **bike** has a custom look, with a visible exhaust system that includes a rusted section, giving it a vintage or modified appearance. The tires are thick and designed for grip, suitable for various terrains. ...

Prompt:

Describe this image in detail.



Qwen2.5-VL (Deco) :

...The motorcycle has a unique and rugged design, featuring a large front headlight, a prominent air filter, and exposed engine components that give it a raw, industrial look. The exhaust pipes are visible and appear to be made of metal, adding to the bike's aggressive aesthetic. The tires are wide and robust, suitable for off-road or touring conditions. The **bike** also has panniers mounted on either side, suggesting it might be used for long-distance travel or carrying gear. The lighting in the photo is bright, indicating it was taken during the day under sunny conditions. The background consists of lush trees and foliage, which adds a natural and serene backdrop to the dynamic scene of the motorcyclist in motion.

Qwen2.5-VL (SAKED) :

...The motorcycle itself is a sleek, modern design, with a visible front headlight and a robust, muscular engine. It has a classic, vintage-style aesthetic, with a chrome and black color scheme. The exhaust system is visible, and it appears to be a dual-pipe setup. The rider's posture is leaned slightly into the turn, which is evident by the angle of the front tire and the position of the body. The background is a natural, outdoor setting with lush greenery, including trees and bushes, which suggests a rural or countryside location. The lighting is bright, indicating that it is either mid-morning or early afternoon. The overall impression is of an active, outdoor activity, likely a solo ride or a solo road trip. The focus is on the interaction between the rider and the motorcycle, as they navigate the environment.

Qwen2.5-VL (Greedy) :

...She is holding the spool of kite string in both hands, which is attached to a colorful kite flying high above her. The kite appears to be triangular-shaped with bright colors, including red, yellow, and blue. The beach is wide and stretches out towards the ocean, where gentle waves can be seen rolling onto the shore. In the background, there are a few people and structures, possibly houses or beach **umbrellas**, indicating that it might be a popular spot for beach activities. ...

Qwen2.5-VL (Deco) :

...She is holding the spool of kite string in both hands, which is attached to a colorful kite flying high above her. The kite appears to be triangular-shaped with bright colors, including red, yellow, and blue. The beach is wide and stretches out towards the ocean, where gentle waves can be seen rolling onto the shore. In the background, there are a few people and structures, possibly houses or beach **umbrellas**, indicating that it's a popular spot for leisure activities. The overall atmosphere of the image is serene and joyful, capturing a moment of simple outdoor fun.

Qwen2.5-VL (SAKED) :

...She is holding a blue and white spool of kite string, which is being used to control the kite that is flying in the sky. The kite itself is a vibrant, multi-colored design, with a triangular or diamond shape, and it is visible in the upper part of the frame. The background of the image is a vast, open beach with a clear, light blue sky overhead. There are a few scattered clouds but overall, the weather seems to be calm and pleasant. The shoreline is visible, with some small waves gently lapping against the shore. In the distance, a few people can be seen either sitting or walking on the beach, but they are not the focus of the image. The overall impression is one of a relaxed, enjoyable day spent outdoors, with the focus on the simple joy of flying a kite.

Prompt:

Describe this image in detail.



Qwen2.5-VL (Greedy) :

...The cat has striking yellow eyes, which stand out against its fur. Its face is predominantly white with a black patch over one eye, giving it a distinctive appearance. The cat's expression appears calm and slightly curious as it looks directly at the camera. The background includes some blurred objects, possibly **books or boxes**, suggesting that the photo was taken indoors, perhaps in a home setting. The overall tone of the image is warm and playful due to the cat's attire and the soft lighting.

Qwen2.5-VL (Deco) :

...The cat's expression appears calm and slightly curious as it looks directly at the camera. The background includes some blurred objects, possibly **books or boxes**, suggesting that the photo was taken indoors, perhaps in a home setting. The overall tone of the image is warm and playful due to the cat's attire and the soft lighting.

Qwen2.5-VL (SAKED) :

...The most notable feature of this image is that the cat is wearing a small, bright pink knitted hat. The hat is snugly fit, and it has a slightly oversized, slightly comical look that adds a touch of humor and charm. The hat also has a small, round, fuzzy pom-pom on the top, which further accentuates the playful nature of the scene. The background of the image is somewhat blurred, but it seems to be an indoor setting, possibly a home or a similar environment. There are some indistinct objects, such as a pink and other colorful items, which might be part of a room or a personal space. The overall impression is that of a lighthearted and fun moment captured in a domestic setting.



Figure 10. Qualitative visualization results on Qwen2.5VL using different decoding methods, with hallucinated content highlighted in red.

Prompt:

Describe this image in detail.



InternVL3-8b (Greedy) :

The image shows a bathroom with two toilets positioned side by side. Both toilets have white ceramic tanks and **bowls**. The floor is tiled with a combination of brown and beige square tiles. The walls are covered with white square tiles. Above the toilets, there is a metallic grab bar installed on the wall, likely for support. The toilets appear to be standard models, and the bathroom has a clean and functional appearance.

InternVL3-8b (Deco) :

The image shows a bathroom with two toilets positioned side by side. Both toilets have white ceramic tanks and **bowls**. The floor is tiled with a combination of brown and beige square tiles. The walls are covered with white square tiles. Above the toilets, there is a metallic grab bar installed on the wall, likely for support. The toilets appear to be standard models, and the bathroom has a utilitarian, clean appearance.

InternVL3-8b (SAKED) :

The image shows a public restroom with two side-by-side toilets. Both toilets are white and have their lids open. The floor is covered with square tiles in various shades of brown and tan, creating a checkerboard pattern. The walls are lined with white tiles, and there is a metal grab bar mounted on the wall above the toilets, likely for support. The overall appearance is clean and functional, typical of a public or institutional restroom.

InternVL3-8b (Greedy) :

The image shows a woman standing next to a decorative clock post. The clock is adorned with a festive wreath and a large red ribbon, suggesting a holiday theme. The clock face is white with black Roman numerals, and it is mounted on a black pole wrapped with red lights. The woman is wearing a dark jacket, light-colored shirt, and dark pants, and she is holding a handbag. The scene is set at night, with streetlights and Christmas lights visible in the background. There are parked cars and **a few people** walking in the distance, adding to the urban nighttime atmosphere.

InternVL3-8b (Deco) :

The image shows a woman standing next to a decorative clock post. The clock is adorned with a festive wreath and a large red ribbon, suggesting a holiday theme. The clock face is white with black Roman numerals, and it is mounted on a black pole wrapped with red lights. The woman is wearing a dark jacket, light-colored shirt, and dark pants, and she is holding a handbag. The scene is set at night, with streetlights and Christmas lights visible in the background. There are parked cars and **a few people** walking in the distance, adding to the urban nighttime atmosphere.

InternVL3-8b (SAKED) :

The image features a woman standing next to a large, decorative outdoor clock. The clock is adorned with a festive wreath and a large red ribbon, suggesting a holiday or celebratory theme. The clock's face is visible, showing it's likely nighttime due to the surrounding darkness and the presence of lights in the background. The woman is dressed in a dark jacket and pants, and she is holding a small bag. She is positioned on a sidewalk near a parking area, where several cars are visible. In the background, there are more lights, possibly from a nearby street or festive decorations. A person is also seen walking away in the background, and there are some buildings or structures nearby. The overall atmosphere is festive and likely during a holiday season.

Prompt:

Describe this image in detail.



Prompt:

Describe this image in detail.



InternVL3-8b (Greedy) :

The image shows an airport baggage claim area. In the center, there is a large flat-screen television displaying a promotional video for Arizona. **The video shows a person snowboarding or skiing down a snowy slope**, with the word "ARIZONA" prominently displayed at the top of the screen. In front of the television, there is a sign with information about baggage claim services. The sign is white with green and black text, detailing the services and possibly fees or instructions for passengers. The floor is covered with a patterned carpet, and the area is well-lit with overhead lights. In the background, there are more screens and possibly other airport signage, though they are not the focus of the image.

InternVL3-8b (Deco) :

The image shows an airport baggage claim area. In the center, there is a large flat-screen television displaying a promotional video for Arizona. **The video shows a person snowboarding or skiing down a snowy slope**, with the word "ARIZONA" prominently displayed at the top of the screen. In front of the television, there is a sign with a list of services and prices, likely related to baggage handling or airport services. The carpeted floor has a patterned design, and the area is well-lit with overhead lights. In the background, there are more screens and counters typical of an airport setting. The overall atmosphere is calm and spacious.

InternVL3-8b (SAKED) :

The image shows a large, flat-screen television in a public space, likely an airport or similar transit area. The TV is displaying a scene from a video or advertisement, featuring a person who appears to be engaging in a water sport, possibly a type or similar activity. The word "ARIZONA" is prominently displayed at the top of the screen, suggesting a promotional or travel-related theme. In the foreground, there is a sign with a list of services or information related to baggage handling. The sign is mostly text, with some small details and possibly some pricing or instructions. The surrounding area has a patterned carpet, and there are other similar screens in the background, likely for similar purposes.

Figure 11. Qualitative visualization results on InternVL3 using different decoding methods, with hallucinated content highlighted in red.